A Smart Experimental Setup for Vibration Measurement and Unbalance Fault Detection in Rotating Machinery

Guilherme Kenji Yamamoto, Cesar da Costa, João Sinohara da Silva Sousa

***Abstract*— Rotor unbalance is the most common cause of machine vibrations; thus, most rotating machinery problems can be solved by balancing the rotor to correct the misalignment. Imbalance problems in rotary machine motors can be extremely frustrating to users and may lead to greatly reduced reliability. It is imperative that downtime is avoided or minimized for all operations and manufacturing processes. In practice, rotors can never be perfectly balanced owing to manufacturing errors such as porosity in casting, non-uniform density of materials, manufacturing tolerances, and the gain or loss of material during operation. As a result of mass unbalance, a centrifugal force is generated, which must be counteracted by bearings and support structures. Over the past few years, there have been major technological developments in digital signal processing, embedded systems, field programmable gate arrays, computers, and instrumentation, including innovations in both hardware and software. Such innovations have allowed the development of new methods of fault detection and diagnosis for rotating machinery. This paper presents a smart experimental method for vibration measurement and unbalance fault detection in rotating machinery.**

***Index Terms*— Rotating electrical machine; Diagnostic; Fault; Vibration; Digital signal processing.**

I. INTRODUCTION

Balancing motors are required on all types of rotating machinery, including motors, to obtain smooth-running machines. This process is performed in a factory on a balance machine at a precision level determined by the motor speed, size, and vibration requirements. The highest precision is required for two-pole motors. Two-pole and large four-pole motors should be balanced at their operating speed in the balance machine. The assembled motors are then run in a test to confirm that the vibration requirements are met in operation. Although they do not usually directly concern the user, a few salient factors affecting factory balance will be discussed here. These mainly apply to two-pole motors. Most medium-to-large motors are used for constant-speed applications, although there has been a recent increase in the number and size used for variable-speed applications on adjustable-speed drives. Constant-speed motors need to be precision-balanced only at one speed, namely, their operating speed. Variable speed applications require that good rotor balance be maintained throughout the operating speed range, which may typically be from 40% to 100% of their synchronous speed [1,2,3].

Rotor balance involves the entire rotor structure, which is made up of a multitude of parts, including the shaft, rotor laminations, end heads, rotor bars, end connectors, retaining rings (where required), and fans. The design and manufacture of these components must be controlled for achieving stable precision balance. Specifically, the following must be taken into account: (i) parts must be precision manufactured for to ensure close concentricities and to minimize individual unbalance; (ii) loose parts, which can result in shifting during operation, causing a change in balance, must be avoided or minimized; and (iii) balance correction weights should be added at or near the points of unbalance [4,5].

Rotor imbalance causes reaction force generation in the coupling, which are often a major cause of machinery vibrations. Szabo [6] first evaluated the unbalanced forces generated in a rotor shaft and showed the presence of levels of first (x1) and second (2x) harmonic vibration responses. Different methodologies based on vibration spectral analysis have been proposed using fast Fourier transform (FFT) [7,8]. Bossio et al [9] studied angular misalignment and unbalance in induction motors with flexible couplings. Tallam et al [10] investigated the load unbalance and shaft misalignment using stator current in inverter-driven induction motors. Unbalance and misalignment have been analyzed, as shown in the work of Martinez-Morales et al [14], using data fusion for multiple mechanical fault diagnosis in induction motors. Quiao et al [15] reported that imbalance faults constitute a significant portion of all faults in wind turbine generators (WTGs). Historically, vibration monitoring techniques have been widely used for the diagnosis of unbalance faults in induction motors, but, as reported by Kucuker et al [16], electrical detection methods have been preferred in recent years.

The contribution of this work is the development of a smart experimental setup with an FPGA-based signal processor that uses a parallel architecture for multiple-signal processing to combine vibration and FFT analyses and thus perform online unbalance and mechanical faults condition in an induction motor.

II. VIBRATIONS OF ROTATING MACHINES

A vibration is the movement of a physical quantity in relation to a reference location in a cyclically increasing and decreasing manner as a function of time. The most important features of machine vibrations change according to Equation

Manuscript received May 20, 2016

Guilherme Kenji Yamamoto, Pos graduation Department, IFSP – Federal Institute of Sao Paulo, SP, Brazil
Cesar da Costa, Pos graduation Department, IFSP – Federal Institute of Sao Paulo, SP, Brazil
Joao Sinohara da Silva Souza, Pos graduation Department, IFSP – Federal Institute of Sao Paulo, SP, Brazil

1. Fig. 1 illustrates the behavior of Equation 1 in the time domain [6].

$$x(t) = A.sen(wt + \phi) \quad (1)$$

Where

A - Amplitude (mm/sec);
w - Angular frequency (1/sec);
φ - Initial phase angle constant.

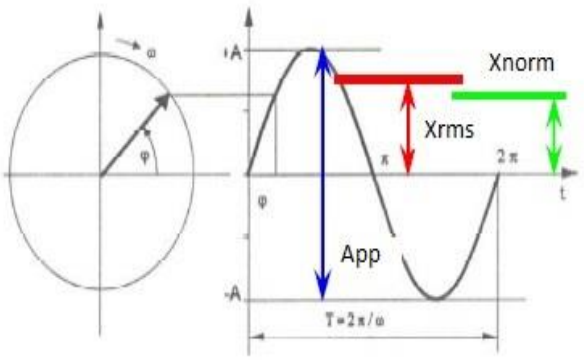

Figure 1. The characteristic quantities of signal vibrations

III. UNBALANCE AND MECHANICAL FAULTS

The unbalance is the source of vibration commonly found in rotating machinery. It is a very important parameter, which must be carefully taken into account in the design of modern machines, especially for applications involving a high degree of reliability and machines that operate at high speeds. Mathematically, the unbalance can be expressed as follows [11]:

$$\vec{U} = m \times \vec{r} \ [\text{g mm}] \quad (2)$$

Where

m = unbalanced mass (in g);
r = distance of the unbalanced mass in relation to the center axis (in mm).

The centrifugal force imbalance that generates vibration is expressed as:

$$\vec{F} = m \times \vec{r} \times w^2 \ [\text{N}] \quad (3)$$

Where

F = force in Newtons (N);
m = unbalanced mass (in g);
r = distance of the unbalanced mass in relation to the center axis (in mm);
w = speed in radians per second (rad/sec).

The specific unbalance is calculated as follows:

$$\vec{e} = \frac{m\vec{r}}{M} \quad [\text{g mm /kg}] = [\ \mu m\ ] \quad (4)$$

The most common types of unbalance in rotating machinery are: (i) static; (ii) coupled; (iii) quasi-static; and (iv) dynamic.

A. The Static Unbalance

The static unbalance is defined as the eccentricity relative to the center of gravity of a disk, caused by a point mass at a certain radial distance from the rotation center, as shown in Fig. 2. A mass equal value, set at an angle 180° with respect to the unbalancing at the same distance in radians, is required to restore the center of gravity to the same point of the center of rotation. The static balancing involves first resolving the forces in a plane and adding a correction mass in this same plane. Rotating parts which have many masses concentrated in only one plane can be treated in the same way as static balancing problems. If the disc has a diameter of between seven to ten times its width, it is usually treated as a disk with a single plane [11]. The static unbalance method was used in this work.

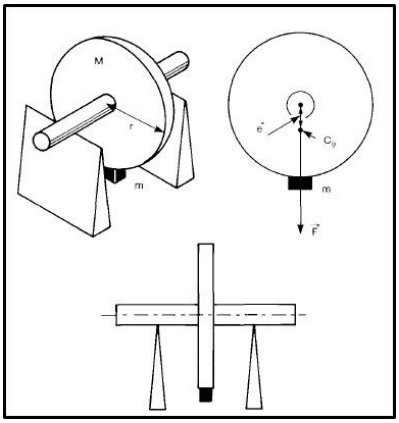

Figure 2. Schemes of the static unbalance [11].

IV. PROPOSED METHODOLOGY

Previously, the diagnosis of shaft unbalance conditions was mainly performed using vibration analysis. In this study, the authors have investigated the unbalance effect on the rotor shaft using both the vibration characteristics and a smart experimental setup based on an algorithm embedded on FPGA. This work proposes the detection and correction of static unbalance.

A. Experimental Procedure

The experiment was conducted with a smart experimental setup (Figure 3) that possessed (1) a 3-phase induction motor (0.25 cv, 4 polos, 1710 rpm); (2) a variable speed controller with voltage vector control; (3) an experimental rotor for the test, which consists of one disk of 90 mm in diameter and 12 mm in thickness, into which holes were inserted for the introduction of the unbalance fault; (4) a shaft with 8 mm in diameter and 250 mm in length; (5) rolling bearings; (6) ball bearings, with a reference frequency of 38,000 rpm and a dynamic load of 351 kgf; (7) a helical coupling, allowing an angular misalignment of 5° at a reference frequency of 25,000 rpm and a rated torque of 2.3 Nm; (8) a sensor ceramic piezoelectric accelerometer with a sensitivity of 1.02 mV/(m/s) and a frequency range from 0.3 to 15,000 Hz; (9) a photoelectric sensor for monitoring the phase and frequency of the shaft rotation; (10) the CompactRIO hardware architecture with a real-time processor and an FPGA chip; and (11) a PC running the application software in LabVIEW.

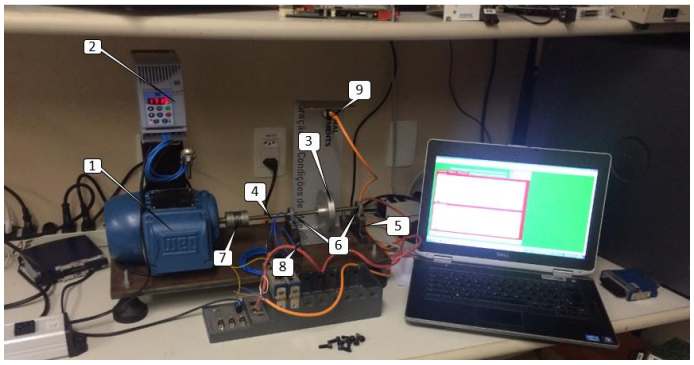

Figure 3. Experimental setup.

B. *Proposed Algorithm Embedded in FPGA*

The block diagram of the algorithm embedded in the FPGA is shown in Figure 4. The different stages of the proposed system are discussed here.

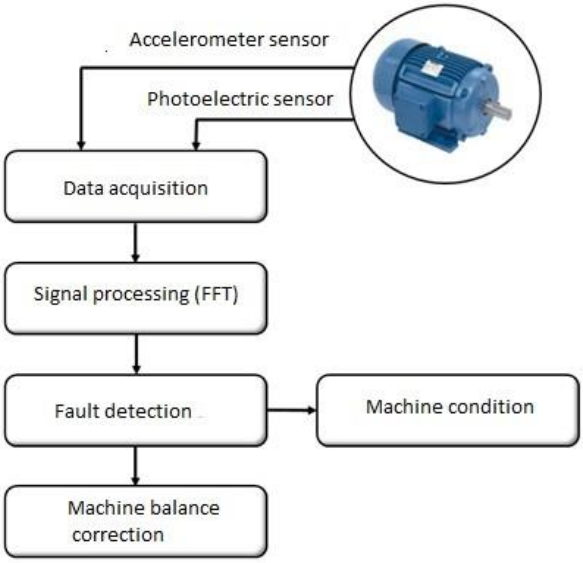

Figure 4. Block diagram representing the algorithm for automatic fault unbalance detection and its correction.

C. *Data Processing*

The hardware platform CompactRIO, based on FPGA technology, was used for the acquisition, monitoring, analysis, and processing of signals from the smart experimental setup. The CompactRIO hardware architecture combines three components: (i) a real-time processor to the system CPU; (ii) an FPGA chip embedded in the structure; and (iii) space for accommodation of up to eight modules of inputs and outputs (accelerometer and photoelectric sensors). The model used was the NI 9074, which is based on FPGA, and the real-time operating system is the physical interface with the sensors, which is required to condition the signals, perform the data acquisition and analysis, and process the essential calculations for the mathematical application software.

E. *Application Software*

The application software is divided into two algorithms: (i) detection of unbalance faults and (ii) calculation of the trial mass and its position on the disk for unbalance correction.

F. *Unbalance Fault Detection - Algorithm*

The data from the accelerometer (vibration signal) and photoelectric (speed rotor signal) sensors are acquired for signal processing. The vibration due to the unbalance is seen as a peak in the spectrum at the vibration frequency. The vibration level and the phase of the rotational frequency of the rotor signal can be read directly from the display. Fig. 5 shows the proposed methodology, which combines the vibration and rotational frequency signals of the rotor analyses to precisely determine the motor condition by the following procedure:

1) Acquisition of the vibration and rotational frequency signal during the induction motor operation;

2) Processing of the vibration signal using the FFT;

3) Processing of the vibration signal and the rotation frequency signal in the time domain to determine the phase angle between the signals;

4) From the results of these analyses (steps 2 and 3), to determine whether the motor condition is balanced or unbalanced;

5) If the motor condition is unbalanced, determine the trial mass and the position it neds to occupy on the disk to correct the unbalance.

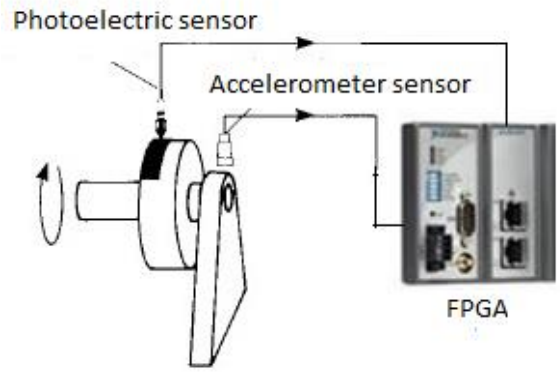

Figure 5. Acquisition of the vibration and rotational frequency signal.

G. *Unbalance Correction Algorithm*

The unbalance correction algorithm used is based on vector diagram calculations in single-plane balancing. The values of the correction mass and angle can be determined by representation the measurements vectorially, as shown in Fig. 6.

1. A vector $\vec{V}_0$ is drawn representing the initial unbalance. The length of $\vec{V}_0$ is equal to the vibration amplitude, and its direction is given by the phase angle, as shown in Figure 6a.

2. Another vector $\vec{V}_1$ is drawn representing the amplitude and phase measured with the trial mass mounted, as shown in Figure 6b.
3. The tips of vectors $\vec{V}_0$ and $\vec{V}_1$ are joined by means of a third vector $\vec{V}_T$, which is marked so that it indicates the $\vec{V}_0$ to $\vec{V}_1$ direction, as shown in Figure 6c. This vector represents the effect of the trial mass alone.
4. A vector is drawn parallel to vector $\vec{V}_T$, with the same amplitude and direction, but starting at the origin. This vector is also called $\vec{V}_{T'}$, as shown in Figure 6d.
5. The vector $\vec{V}_0$ is continued through the origin, in the opposite direction to $\vec{V}_0$. This vector is called $\vec{V}_C$, and it represents the position and magnitude of the mass required to counteract the original unbalance, as shown in Figure 6e.
6. If we assume that the amplitude of the vibration is proportional to the unbalanced mass, we obtain the relation:

$$\frac{M_T}{\vec{V}_T} = \frac{M_C}{\vec{V}_C} = \frac{M_0}{\vec{V}_0} \quad (5)$$

$$M_C \Rightarrow M_0 = \frac{|V_0|}{|V_T|} \times M_T \quad (6)$$

7. Equation 6 enables us to find the value of the compensating mass, M_C.
8. The position of the mass relative to the position of the trial mass can be determined from the vector diagram using Equation 7.

$$\phi_C = \phi_T + \phi_0 + 180^0 \quad (7)$$

The calculated angle is measured from the position marked on the rotor indicating the point where the trial mass was mounted. If it is a positive angle, it is measured in the direction of rotation. A negative angle is measured in the opposite sense.

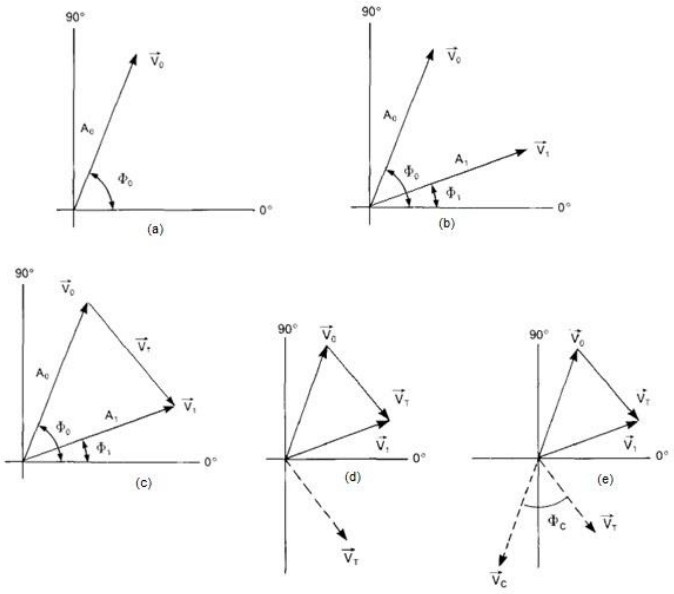

Figure 6. Vectors diagram calculations: (a) the vector of the initial unbalance; (b) the vector of the measured amplitude and phase; (c) the third vector of the effect of the trial mass; (d) the vector parallel; and (e) the vector of the position and magnitude of the mass [11].

The described algorithms were developed in the LabVIEW real-time software and later embedded in the FPGA reconfigurable, as shown in Fig. 7.

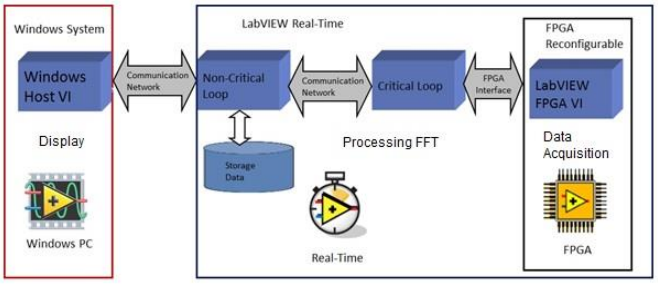

Figure 7. Algorithm Implementation into FPGA

V. RESULTS AND ANALYSIS

The induction motor was operated at a constant speed of 28.5 Hz (1710 rpm). The vibration and rotational frequency signal of the system were recorded by an accelerometer sensor (vibration signal) placed in the vertical direction and a photoelectric sensor (rotational speed signal) placed next to the disk.

The experiments were first performed with the balanced disk. The required unbalance was then induced in the rotor shaft by the addition of the trial mass on the disk, as explained in the previous section. Experimental studies confirm that the rotor unbalance creates a vibration frequency equal to the rotational speed, with amplitude proportional to the amount of unbalance [12, 13]. A series of tests, described hereafter, were performed in order to focus on the relevant information in the spectrum and be able to discriminate the unbalance fault component.

A. *Machine Reference Running Balanced*

In the first trial, the machine worked without the addition of mass to the disk, and was therefore considered balanced. Figure 8 shows the signal acquired by the photoelectric sensor, which was used to determine both the engine rotation frequency and the lag angle for the vibration signal.

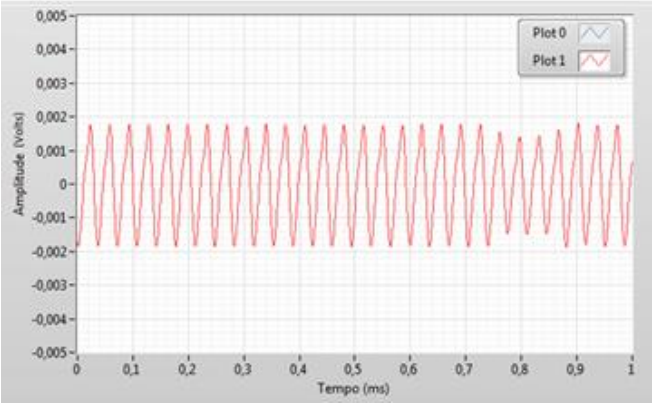

Figure 8. Signal of photoelectric sensor with balanced condition.

Figure 9 shows the time-domain vibration signal obtained by the accelerometer sensor for an unflawed, balanced engine. The signal's peak amplitude was approximately 0.50 mV. For this balanced condition, the phase angle between the photoelectric sensor signal and the accelerometer would be equal to zero.

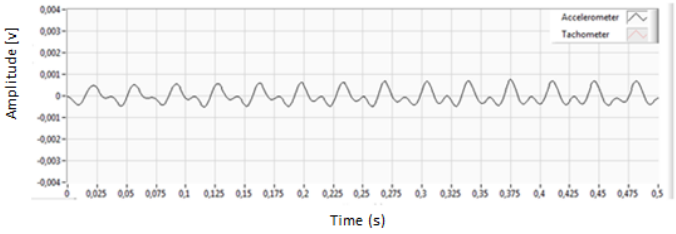

Figure 9. Signal of accelerometer sensor with balanced condition

Figure 10 shows the FFT result, which can be used to determine the magnitude of the signal in the frequency domain. The data contained in the vibration spectrum are processed by the system to identify unbalance failures. The signal of interest is given by the motor rotation frequency (28.5 Hz); no unbalance is detected, and the signal magnitude is 0.20 mV.

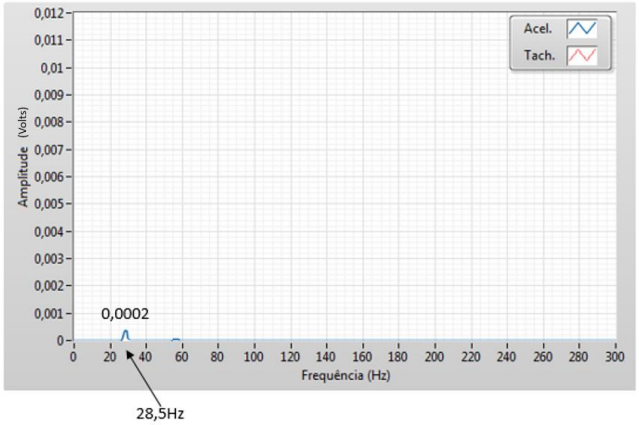

Figure 10. Vibration spectrum with balanced condition

B. *Machine Running with One Mass Attached*

To perform the unbalance fault simulation, a trial mass of a pre-determined weight was inserted, as shown on the Fig. 11. In the first experiment, a mass of 0.006 kg attached to the rotor shaft disc, was inserted. The unbalance thus created produced a mechanical vibration in the machine's structure.

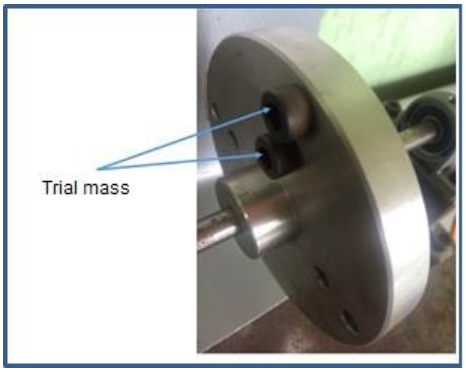

Figure 11. Rotor shaft disc with trial mass

Figure 12 shows the time-domain vibration signal for a faulty unbalanced machine; an increase in the peak amplitude signal from 0.50 to 5.5 mV can be observed. This unbalance produced an increase in the machine's vibration level. For this unbalanced condition, the phase angle between the signal of the photoelectric sensor and the accelerometer is calculated to be approximately 8.5º.

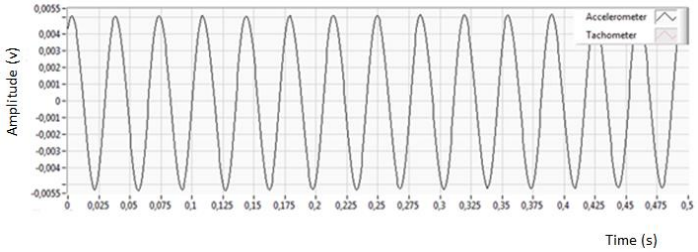

Figure 12. Vibration signal with one trial mass.

Figure 13 shows the spectrum of the vibration motor signal with a test mass. The signal of interest is given by the motor rotation frequency (28.5 Hz); an unbalance fault is detected by an increase in the spectrum amplitude (from 0.20 to 5.6 mV).

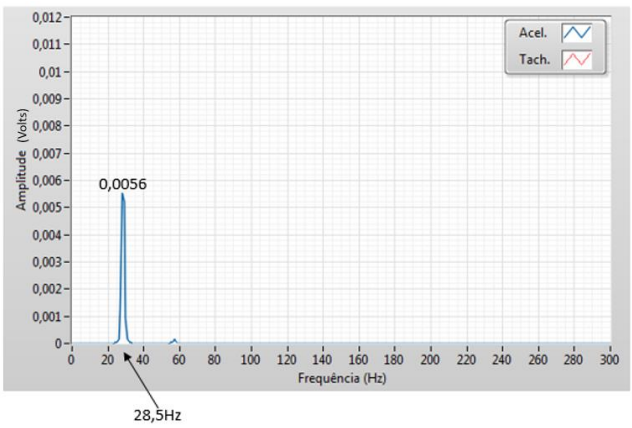

Figure 13. Vibration spectrum measured by accelerometer for one unbalancing mass attached to the rotor shaft disc

C. *Machine Running with two Mass Attached*

With the objective of validating the unbalance detection by using the vibration spectrum, a final experiment was performed by inserting two unbalancing masses of 0.006 kg each, attached to the rotor shaft disc. As shown in Fig. 14, the magnitude of the vibration spectrum is 11.2 mV (an increase of approximately 56 times compared to the vibration spectrum of the balanced machine shown in Figure 10).

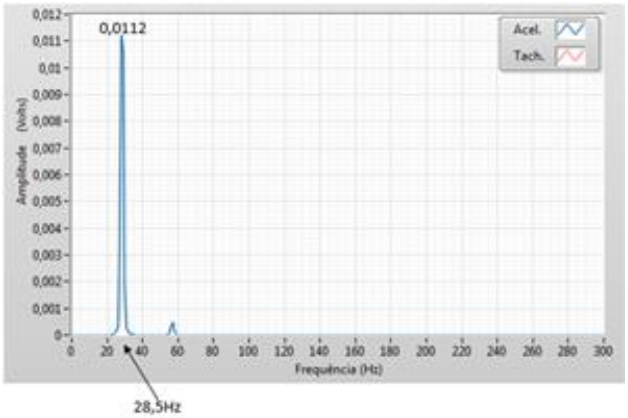

Figure 14. Vibration spectrum measured by accelerometer for two unbalancing masses attached to the rotor shaft disc.

D. *Balancing the Shaft Rotor Process*

We implemented the unbalance correction algorithm after identifying the correlation between the unbalance and the increase in the vibration amplitude.

To define the value of the correction angle ($\emptyset_C$) and mass of correction (Mc), the values of the phase angle and magnitude from V0 and V1 must be calculated. During the balancing process, two pieces of data are logged in the system memory: (i) Vector V0, referred to as the initial vibration, and (ii) Vector V1, referred to as the loading of trial masses. Once V0 and V1 have been calculated and the weight of the trail mass has been inputted to the software, it is possible to calculate the correction mass, and its position can be attached to the rotor shaft disc.

We also report further experiments that validate the proposed procedure by proving its effectiveness at balancing the system. Table 1shows four experiments in which different masses were used for the unbalance and trial masses.

We chose the results presented in Experiment 3, Table 1, to validate the unbalance correction process (inserting a new correction mass positioned on the disc axis) using the proposed system.

The correction process includes removing the 0.0055 kg test mass and inserting a 0.0039 kg correction mass at 86.3° (calculated by the system) in the direction of the motor rotation. The results of this are shown in Figure 15, which superimposes vibration signals from the initial 0.006 kg mass with those corresponding to the fixed 0.0039 kg correction mass.

	Test 1	Test 2	Test 3	Test 4
Machine speed (rpm)	1710	1710	1710	1710
Unbalance Mass, M_0 (kg)	0.003	0.0055	0.006	0.008
Unbalance Vector Vibration, V_0	0.0019	0.0043	0.0031	0.0047
Unbalance Angle,$\angle_0$(°)	114.5	288	8.5	6
Trial Mass, M_T (kg)	0.0042	0.008	0.0055	0.0030
Trial Vector, V_T	0.0038	0.0072	0.0058	0.0059
Trial Angle,$\angle_T$(°)	66.3	333.5	314.6	32.6
Correction Mass, M_C (kg)	0.0027	0.0065	0.0039	0.0057
Correction Angle,$\angle_C$(°)	78	81.2	-86.3	77.7

Table 1: Experimentally obtained correction unbalance data

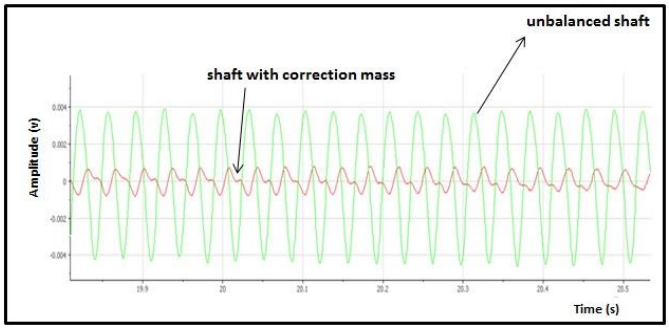

Figure 15. Comparing the vibration signal for the unbalance shaft with the shaft with correction mass

VI. CONCLUSION

The implementation of a smart experimental setup with an FPGA-based signal processor that combines vibration and FFT analyses presented satisfactory results when performing online unbalance and mechanical fault identification in an induction motor.

For a constant motor rotation frequency (28.5 Hz), a comparison between the vibration levels in the time domain and their respective frequency spectra reveals a significant increase in amplitudes for all three tests as the machine unbalance increases.

Practical experiments using the "Smart Experimental Setup" show that adding a correction mass at the location indicated by the system made it possible to effectively reduce the vibration caused by unbalance to levels similar to those of a balanced rotating machine.

The proposed smart experimental setup for vibration measurement and unbalance fault detection in rotating machinery has been successfully tested and is ready for application in 'real world' systems.

REFERENCES

[1] Surendra N. Ganeriwala (Suri), Brian Schwarz & Mark H. Richardson, "Using Operating Deflection Shapes to Detect Unbalance in Rotating Equipment" . Journal Sound and Vibration 43 (5), May 2009.
[2] Ganeriwala, Surendra N., Li, Zhuang, Richardson, Mark, "Using Operating Deflection Shapes to Detect Shaft Misalignment in Rotating Equipment," Proceedings of International Modal Analysis Conference (IMAC XXVI), February, 2008
[3] M. Benbouzid and G. Kliman, "What stator current processing based technique to use for induction motor rotor faults diagnosis", *IEEE Trans. Energy Convers.*, vol. 18, no. 2, pp. 238–44, Jun. 2003.
[4] C. Kral, T.G. Habetler, R.G. Harley, "Detection of Mechanical Imbalances without Frequency Analysis", *IEEE Transactions on Industry Applications*, vol. 40, no. 4, pp. 1101–1106, Jul./Aug. 2004.
[5] A.K. Verma, S. Sarangi and M. H. Kolecar, ''Experimental investigations of misalignment effects on rotor shaft vibration and on stator current signature", Journal of Failure Analysis and Prevention, Vol. 14, Issue 2, pp. 125-138.
[6] J.Z. Szabo, ''Vibration diagnostic test for effect of unbalance", INES 2012 - 16th International Conference on Intelligent Engineering System, Lisbon, Portugal, 13-15, 2012,pp. 81-85.
[7] J.Piotrowski, ''Shaft Alignment Handbook", 3rd edn, CRC: New Yorn, 2006.
[8] T. H. Patel, A. K. Darpe, ''Vibration response of misaligned rotor", Journal Sound Vibration 325, pp. 609-628, 2009.
[9] J. M. Bossio, G. R. Bossio, C. H. De Angelo, "Angular misalignment in induction motor with flexible coupling". Proceedings of the IEEE IECON, Porto, Portugal, 3–7 November, 2009, pp. 1033–1038.
[10] R. R. Obaid, T. G. Habetler, R. M. Tallam, "Detecting load unbalance and shaft misalignment using stator current in inverter-driven induction motors".Electric Machines and Drives Conference.IEMDC'03.IEEE Internacional Volume 3, 1-4 June 2003, pp. 1454 – 1458, 2003.
[11] M. MacCamhaoil, "Static and dynamic balancing of rigid rotors", Application note, BruelKjaer, pp.1-20
[12] F. Jiang, W. Li, Z. Wang, and Z. Zhu, "Fault Severity Estimation of Rotating Machinery Based on Residual Signals," Advances in *Mechanical Engineering*, ID 518468, 8 pages, 2012.
[13] H. Bendjama, S. Bouhouche, and M.S Boucherit, "Application of Wavelet Transform for Fault Diagnosis in Rotating Machinery," *International Journal of Machine Learning and Computing*, Vol. 2, No. 1, pp. 82-87. February 2012.
[14] J. D. Martinez-Moralez, E. Palacios, and D. U. Campos-Delgado, "Data fusion for multiple mechanical fault diagnosis in induction motors at variable operating conditions". Proceedings of the 7thInternational Conference on Electrical Engineering, Computing Science and Automatic Control, pp. 176-181, September 2010.
[15] W. Qiao and X. Gong, "Imbalance Fault Detection of Direct-Drive Wind Turbines Using Generator Current Signals". IEEE Transactions on Eergy Conversion, Vol. 27, No. 2, pp. 468-476, 2012.
[16] A. Kucuker and M. Bayrak, "Detection of Mechanical Imbalances of Induction Motors with Instantaneous Power Signature Analysis". Journal Electrical Engineering Technology, Vol. 8, No. 5, pp. 1116-1121, 2013.

Guilherme Kenji Yamamoto was born in São Paulo, Brazil.
He received the B.Eng. degree in electrical engineering from São Judas Tadeu University, São Paulo, Brazil, in 2010, and is currently pursuing the M.Sc. degree at the IFSP - Federal Institute of Education, SP, Brazil. His main research interests are fault detection based on mechanical vibration, embedded systems, rotating machine analysis with special emphasis on fault diagnosis. In 2012, he became a Product Engineer with National Instruments, São Paulo, Brazil, the global leader of software-defined instruments company, where he has focused in activities related with market strategy to create new opportunities in Latin America region.

Cesar da Costa was born in Rio de Janeiro, Brasil.
He received the B.Sc. degree in electronic and electrical engineering from the CEFET- RJ, Federal Center of Technological Education Celso Suckow da Fonseca and Nuno Lisboa University in 1975 and 1980, respectively. He received the M.S. degree in mechanical engineering from Taubate University, São Paulo, Brazil and the Ph.D. degree in Mechanical engineering from UNESP-Universidade Estadual Paulista Júlio de Mesquita Filho, Guaratinguetá, SP, Brazil in 2005 and 2011, respectively. He did Sandwich doctoral stage, PDEE - CAPES, in the IST- Instituto Superior Técnico, Lisbon, Portugal, in 2009. He is currently post doctorate and professor of automation and control engineering in the IFSP - Federal Institute of Education, SP, Brazil. His research interests include Fuzzy controller, machine monitoring, diagnostic, electrical machines and FPGA.
.

João Sinohara da Silva Sousa was born in São Paulo, Brasil.
He received the B. Sc. degree in electronics and electrical engineering from the UNIFEI-MG: Federal University of Itajubá in 1982. He received the M.S. and Ph. D. degrees in automation/production from INPG: Institut Polytechnique of Grenoble, France in 1994 and 1997, respectively. He is currently professor of automation and control engineering in the IFSP: Federal Institute of Education, SP, Brasil and the research, innovation and graduate coordinator in S. J. Campos, SP. His research interests include automation, production systems, computer integrated manufacturing, intelligent control and cyber-dynamic systems.